Adv. Space Res. Vol.1, pp.197-211.
0273-1177/81/0401-0197$05.00/0
© COSPAR, 1981. Printed in Great Britain.

SOME RECENT ADVANCES IN THERMOSPHERIC MODELS

G. Kockarts

Institut d'Aéronomie Spatiale, 3 Avenue Circulaire, B -1180 Bruxelles, Belgium

ABSTRACT

Since the publication of the last COSPAR International Reference Atmosphere (CIRA 1972) valuable progress has been achieved in improving our understanding of the terrestrial thermosphere. As a result, several empirical models are now available for numerous applications. The reliability of these models is discussed within the framework of known physical phenomena. The most recent published advances deal with longitudinal and universal time effects. Some general shortcomings are pointed out in order to stimulate farther progress.

INTRODUCTION

Over a period of three years (1977-1979) five semi-empirical models of the terrestrial upper atmosphere were published in such a way that any potential user could easily compute total densities and temperatures without making use of the COSPAR International Reference Atmosphere [1] . Such a quantitative progress, which also involves a better representation of physical phenomena, implies the necessity for a revision of CIRA 1972. These new semi-empirical models, however, do not necessarily agree with each other for all existing geophysical conditions. This fact will not facilitate the construction and the adoption of a new CIRA, since all available models claim to reproduce observed quantities. The five recent semi-empirical models are designated by the following acronyms : MSIS [2,3] , ESRO4 [4] , J77 [5] , DTM [6] and AEROS [7] . Except for J77, all models are based on spherical harmonic expansions introduced by Hedin et al. [8] in thermospheric modelling.

A systematic comparison between the most recent semi-empirical models will not be undertaken, since such an analysis has been presented by Barlier et al. [9] for MSIS, ESRO4, J77 and DTM and by Jacchia [10] . The thermospheric part of CIRA 1972, which was developed by Jacchia [11] has been compared to DTM and MSIS by Barlier et al. [6] . Nevertheless, some specific discrepancies between the recent models, not shown previously, are pointed out here and a comparison is made for a permanently minor constituent, i.e. atomic nitrogen which is given by Engebretson et al. [12] and by Köhnlein et al. [7] . Finally, the most recent developments dealing with longitudinal effects introduced in MSIS by Hedin et al. [13] and in ESRO4 by Laux and von Zahn [14] are briefly compared.

COMPARISONS BETWEEN MODELS

A perfect model should be able to represent all physical conditions in the past, in the present and in the future. All semi-empirical models are, however, based on a limited set of data. Fig. 1 shows the monthly mean of the 10.7 cm solar flux used as an index under different forms in the models. The period shown covers two solar cycles and its appears immediately that the solar maximum in 1958 was much more intense than the last maximum in 1969. Horizontal lines in Fig. 1 indicate the periods during which different satellites gathered data used in various models. Only drag data leading to total densities are available since the

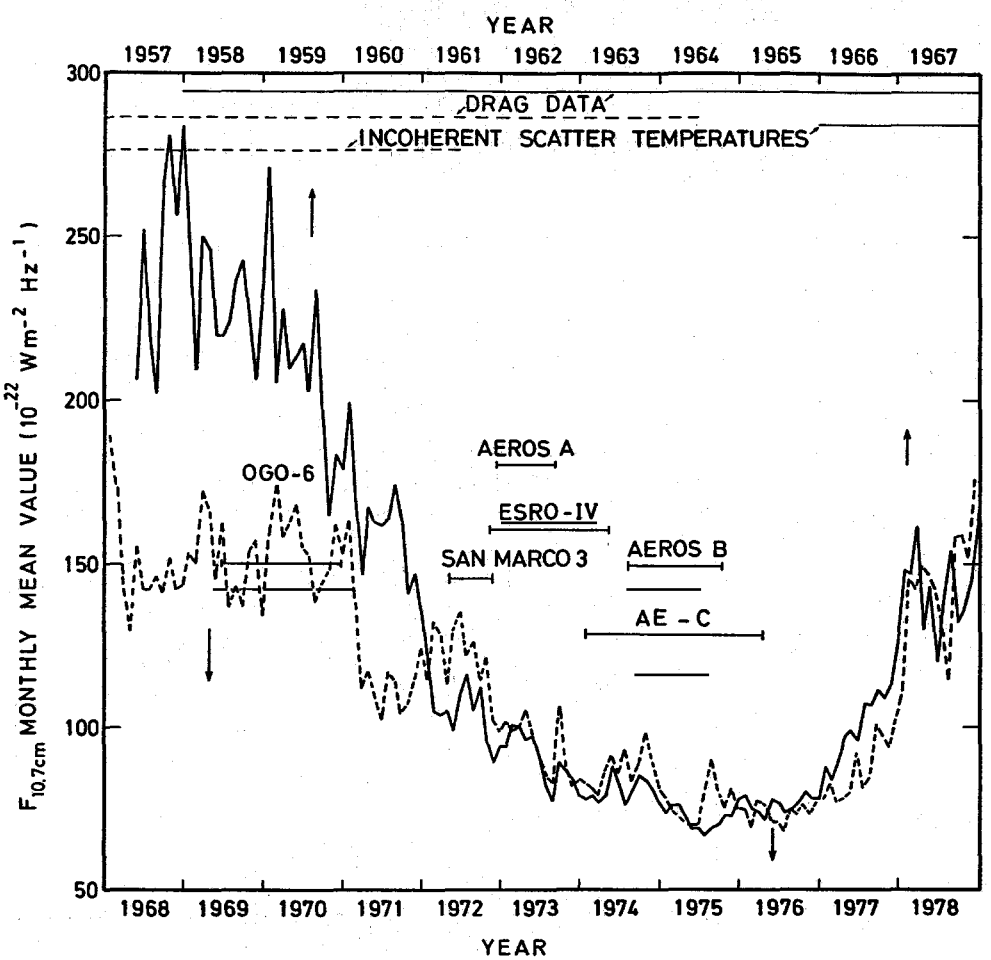

Fig. 1 Monthly mean of the solar decimetric flux as a function of time between 1957 and 1978. Horizontal lines indicate the periods covered by in situ satellite measurements (lower scale) as well as the period during which drag data and incoherent scatter data (upper and lower scale) were used for modeling purposes.

beginning of space age. This type of data is essentially used in two models, i.e. J77 and DTM. All other models are based on much more limited observational periods. This implies that when a spherical harmonic analysis is made, such models lead to extrapolated results when they are applied for geophysical conditions never encountered during the observational periods. It is,therefore,not surprising that a comparison between various models may lead to extreme differences of a factor of two, even in the total densities [9]. Furthermore, even the models J77 and DTM, with the largest data base, covering almost two solar cycles, have difficulties in representing appropriately short term phenomena. All models show different amplitudes in the diurnal variations of the individual components and the phases agree only above 200 km altitude. Incoherent scatter data provided considerable help in improving this situation [15] , particularly with respect to the diurnal temperature maximum.

Since the AEROS model [7] was not available at the time when a systematic comparison between various models was made by Barlier et al. [9] , Fig. 2 shows the annual variation of atomic oxygen concentrations at the geographic poles and at the equator obtained for AEROS, J77 and DTM. Results are given at 300 km

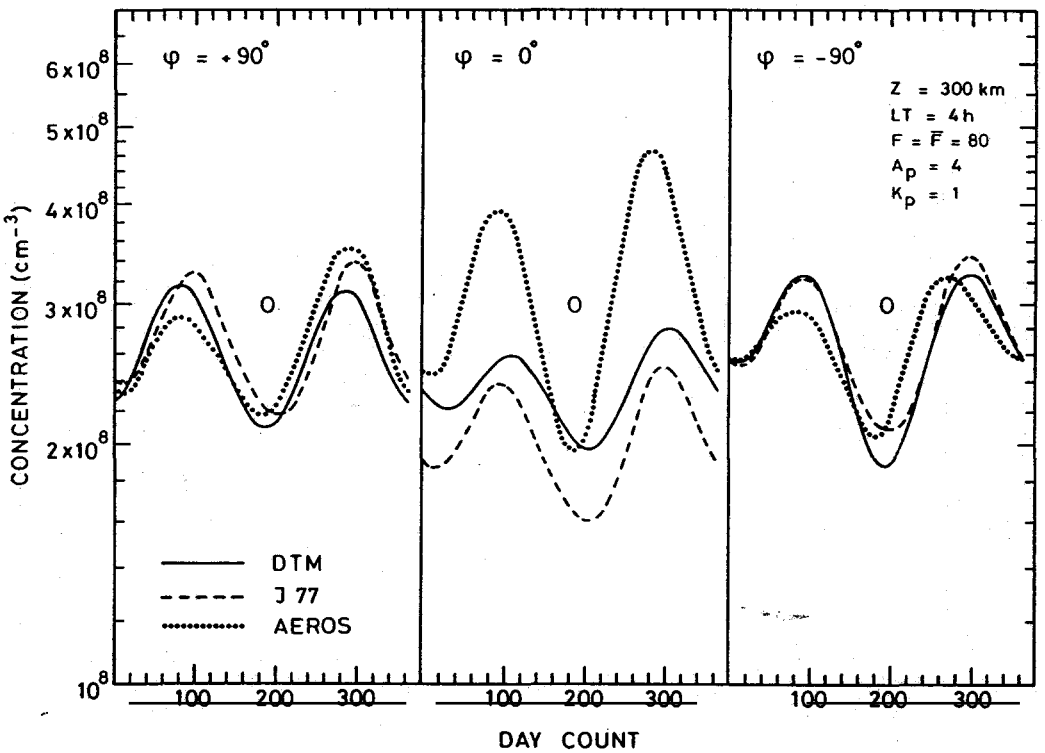

Fig. 2 Annual variation of atomic oxygen at 300 km computed at 4 hours LT with DTM, J77 and AEROS. Three latitudes are represented, i.e. north and south poles and equator. The daily solar decimetric flux F and the mean flux $\overline{F}$ correspond to the average conditions covered by AEROS. Geomagnetic indices are $A_p = 4$ or $K_p = 1$.

altitude for a daily and mean solar decimetric flux $F = \bar{F} = 80 \times 10^{-22}$ Wm^{-2} Hz^{-1} which corresponds to average solar flux conditions during the mass spectrometric measurements used in the construction of AEROS. Quiet geomagnetic conditions ($K_p = 1$ or $A_p = 4$) are adopted and the computations are made for 4 hours local solar time since AEROS data were essentially obtained at 4 hours and 16 hours LT. For this reason, only a cosine term is used in the AEROS model [7] to represent the diurnal variation and this model is probably not appropriate to correctly model the diurnal variation. Köhnlein et al. [7] conclude that the AEROS model is in satisfactory agreement with MSIS and ESR04. Although such a conclusion is also valid for J77 and DTM, it appears, however, in Fig. 2 that significant differences are present in the annual variation of atomic oxygen at the equator. Since atomic oxygen is a major constituent at 300 km altitude, Fig. 2 indicates that for equinox conditions AEROS leads to an equatorial total density which is almost a factor of two higher than in J77 or in DTM. Such a discrepancy cannot be attributed to a systematic difference between drag data and mass spectrometric measurements.

Since the amplitude of the winter helium bulge is not yet well known [9, 16], Fig. 3 shows the annual variation of helium concentrations at 300 km altitude for the same geophysical conditions as in Fig. 2. The amplitude of the bulge is similar in AEROS and in J77, but it is smaller in DTM where only drag data were used.

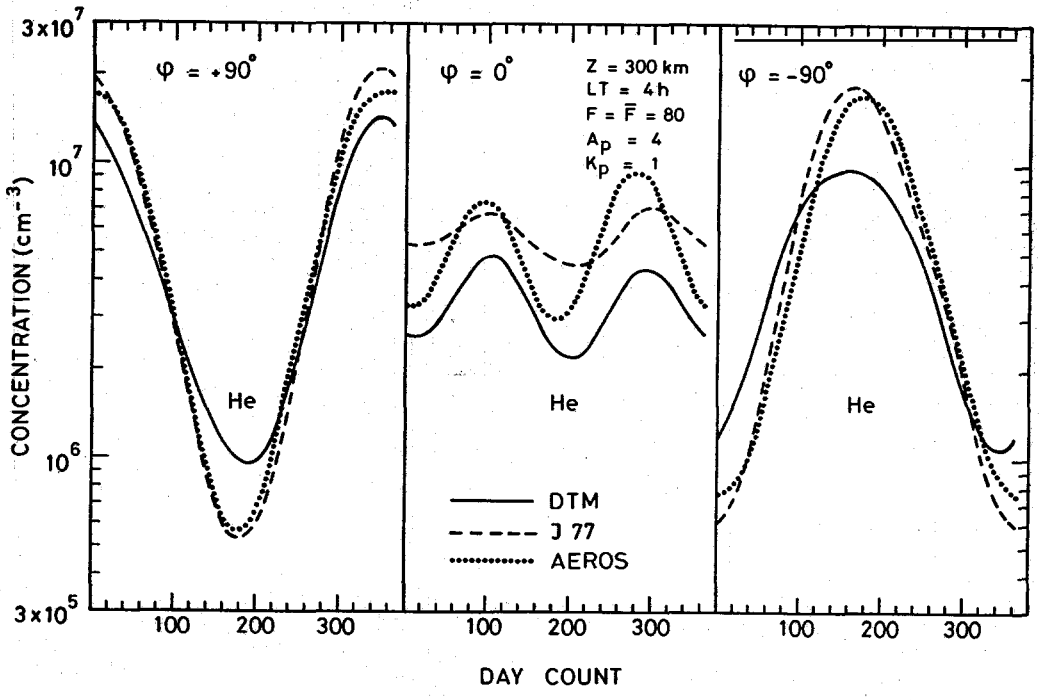

Fig. 3 Annual variation of helium at 300 km for the same geophysical conditions as in Fig. 2.

This remains an open question, although Anderson et al. [17] have shown in an analysis of He 58.4 nm dayglow emissions that both DTM and MSIS in general predict higher helium concentrations than the airglow-determined values. At the equator, the equinoctial maxima for helium are again larger in AEROS than in DTM or in J77, i.e. a situation similar to the atomic oxygen variation shown in Fig. 2. Examples shown in Figs. 2 and 3 indicate that significant differences still exist between the most recent semi-empirical models. When loose expressions like "satisfactory, reasonable or global agreement" are used in model comparisons, great care must be taken in specific applications of semi-empirical models. Even when a model agrees perfectly with a particular observation, it does not imply that the whole model is perfect for other conditions. This is a consequence of the fact that the mathematical formalisms presently used are not necessarily appropriate to represent all physical phenomena in the terrestrial thermosphere. It is even surprising that the use of two indices (solar decimentric flux and geomagnetic index) is sufficient to represent the atmospheric structure with a "reasonable" accuracy. Standard deviations given for a specific model usually represent an internal test for the consistency between the mathematical representation and the limited set of data used for the construction of the model. However, such deviations give no indication of the ability to represent external data not involved in the construction of the model.

EXTERNAL TESTS

Any comparisons between model results and observations not involved in the construction of the model is always a valuable test for the reliability of the model. When such an exercise is made for the diurnal variation of atomic oxygen as deduced by Alcaydé and Bauer [18] from incoherent scatter data, it appears [9] that the amplitude of the diurnal variation is often larger in incoherent scatter data than in any model. This is particularly true for spring conditions at 45°N when the diurnal amplitude in the incoherent scatter data is of the order of a factor of three at 400 km altitude, whereas the largest amplitude in three dimensional empirical models is given by DTM and reaches only a factor of two. Nevertheless, all semi-empirical models are able to reproduce diurnal maxima occuring at different local times for different species. Amplitudes and phases of these maxima should probably be modified if new observational data become available, particularly below 200 km altitude.

Except for J77, all semi-empirical models are characterized by variable lower boundary conditions at 120 km altitude. The J77 model [5] starts at 90 km with constant boundary conditions, but empirical corrections are introduced between 90 km and 120 km to simulate departures from diffusive equilibrium. As a consequence, the concentrations in J77 are also variable at 120 km altitude. Spherical harmonics given at this height in the other semi-empirical models are, however, obtained from data gathered at greater altitudes and model values at 120 km may not necessarily represent real physical conditions, particularly for atomic oxygen which is influenced by photochemical reactions and by transport processes. Recently, Dickinson et al. [19] made a detailed analysis of several rocket flights during which atomic oxygen was measured between 60 km and 140 km using an optical resonance technique at 130 nm. Table 1 gives the measured atomic oxygen concentrations at 120 km for six rocket flights at South Uist (57.4°N, 7.4°W). Data are arranged in seasonal sequence.

TABLE 1 : Atomic Oxygen in (10^{11} cm^{-3}) at 120 km Altitude.

Date	7 Feb 77	11 Feb 77	1 Apr 74	8 Sep 75	29 Nov 74	28 Nov 75
Time (UT)	2309	1359	2237	2355	1153	1256
Dickinson et al. [19]	2.0	2.12	1.67	1.04	0.88	1.26
DTM	0.52	0.66	0.45	0.58	0.81	0.83
J77	0.64	0.72	0.53	0.78	0.84	1.06
MSIS	0.83	0.77	0.73	0.77	0.92	0.87
ESRO4	0.58	0.77	0.41	0.59	0.90	0.93
AEROS	0.68	0.79	0.53	0.72	1.12	1.15

Values obtained from the five semi-empirical models are also indicated and large discrepancies appear between all model values and the measurements. If such a comparison had been made only for the daytime flight on 29 November 1974, we could have stated that a "satisfactory agreement" exists between all models and the measurements. This is actually not the case and our semi-empirical representation of the lower thermosphere is far from being complete.

Since the measurements of Dickinson et al. [19] extend up to 140 km in some cases, Fig. 4 shows relative atomic oxygen concentrations obtained from measurements and from models. For the daytime flight on 11 Feb 1977 all models decrease faster than the observed values, whereas for the nighttime flight on 7 Feb 1977, only J77 is a little outside of the error bar. Dickinson et al. [19] made a similar analysis using CIRA 1972 [1] and concluded that in all cases the discrepancy between model values and the measurements is a consequence of transport phenomena. Above 120 km altitude MSIS is the only model which involves a correction to the usual assumption of diffusive equilibrium. Such a correction never exceeds 13% in Fig. 4 and it is insufficient to bring the daytime MSIS values (almost identical to DTM values) in agreement with the measurements. Model temperatures at 120 km and 150 km are also given in Fig. 4. At 150 km altitudes all models give almost identical temperatures but at 120 km altitude the J77 temperature is always 40 K to 50 K lower than in DTM or MSIS. Furthermore, the discrepancy between measurements and models is always larger for J77. It is therefore possible that the discrepancies shown in Fig. 4 are not due to transport but are an indication that the model temperatures are too low at 120 km altitude. Incoherent scatter temperatures at 120 km above Saint-Santin are actually of the order of 408 K [20] with an amplitude of 15 K for the annual variation and a small negative dependence on solar decimetric flux.

MINOR CONSTITUENTS

Thermospheric minor constituents can be divided in two categories : those which are permanently minor at all heights and those which can become major constituents over certain height ranges as a consequence of diffusive separation in the gravitational field. The first category including argon, carbon dioxide, atomic nitrogen, nitric oxide never influence satellite drag data and they cannot be deduced from such data. The second category deals mainly with atomic oxygen, helium and atomic hydrogen which become successively the major thermospheric component as height increases. Permanently minor constituents are only accessible through selective measuring techniques, such as optical detection or mass spectrometric sampling. A good knowledge of any minor constituent is, however, of paramount importance since fundamental information can be gathered from trace constituents. As an example, mass spectrometric measurements of argon and/or helium

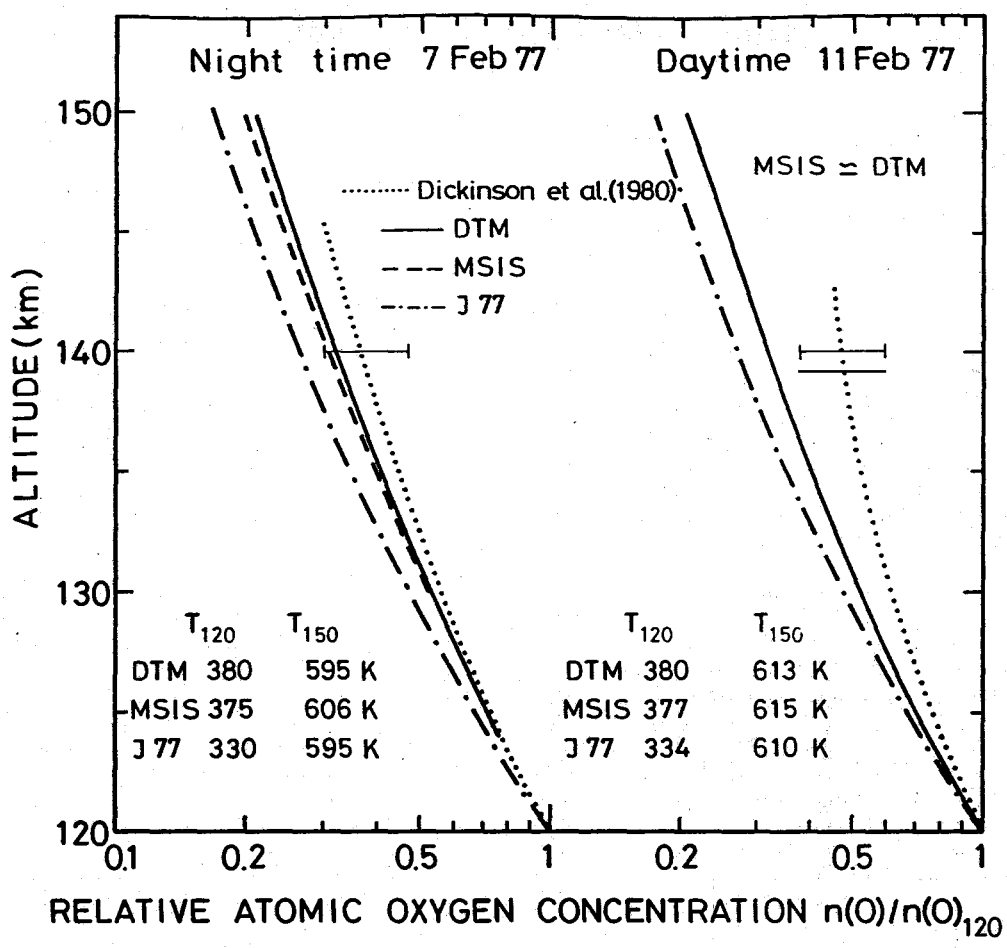

Fig. 4 Vertical distribution of relative atomic oxygen concentrations. Comparison between measured values by Dickinson et al. [19] and model values from DTM [6], MSIS [2,3] and J77 [5] .

provide an excellent tool to investigate the transition from turbulent mixing to diffusive separation in the 100 km altitude region [21] , although other techniques such as sodium clouds ejections [22] and rocket grenade data [23] also contribute significantly to the knowledge of this transition region. Unfortunately, no global coverage is yet available since direct in situ measurements can only be performed by rockets in this height range. Remote sensing from a satellite is probably the only way to solve this question if an appropriate optical technique is developed.

Among the permanently minor constituents, atomic nitrogen is the sole component given by two global models [7, 12] . The first model by Engebretson et al. [12] is based on a spherical harmonic expansion at 375 km altitude using mass spectrometer data from Atmosphere Explorer C during 1974 and part of 1975. Since atomic nitrogen is involved in numerous chemical reactions [24] , its vertical distributions is not necessarily in diffusive equilibrium. It has been shown experimen-

tally [25], however, that atomic nitrogen is in diffusive equilibrium at least above 200 km altitude. Using the Atmosphere Explorer C model at 375 km, it is, therefore, possible to compute atomic nitrogen concentrations at any height above 200 km altitude by adopting a vertical temperature profile. The second atomic nitrogen model is included in AEROS, where the spherical harmonic expansion refers to 120 km altitude for reasons of uniformity with the other constituents. This does not mean that the model can be used at altitudes below 120 km [7]. Figs. 5 and 6 show the annual latitudinal variations of atomic nitrogen at 375 km as given by AEROS [7] and Atmosphere Explorer C [12] for 4 hours and 16 hours local solar times, respectively. These local times have been chosen since they correspond to the local times for which AEROS is the most reliable. Figs. 5 and 6 indicate that the general pattern of the annual variation is similar in both models. However, at 16 hours LT (Fig. 6) the concentrations given by the Atmosphere Explorer C model are approximately a factor of two higher than the values given by AEROS. Even with such differences atomic nitrogen models should be used as upper boundary conditions in a three-dimensional computation of odd nitrogen distributions below 200 km altitude. This could be of some importance for the energy budget of the thermosphere, since it has been shown [26] that nitric oxide is a major cooling agent below 200 km. There is actually a need for the introduction of permanently minor constituents in semi-empirical models in order to improve our knowledge all the physical mechanisms which influence the thermospheric structure.

LONGITUDINAL EFFECTS

The spherical harmonic expansion used in semi-empirical models depends on two angular variables, i.e. geographic latitude and local solar time. The last variable is a consequence of the assumed equivalence between longitude and local time. This implies that the diurnal variation should be exactly identical at any point of a latitudinal circle. However, the geomagnetic effect in J77 is expressed in terms of magnetic latitude and, as a consequence, a longitudinal effect is introduced, since the temperature increase associated with the K_p index is not symetric with respect to the geographic north-south axis. It is, therefore, necessary to specify, in J77, the geographic longitude when comparisons are made with other models. In Figs. 2 and 3 the longitude is 0° for J77, whereas Fig. 4 is constructed for the longitude of South Uist (7.4° W). Thuillier et al. [27] have also introduced the geomagnetic latitude in their temperature model in order to obtain a better representation of the geomagnetic effect at high latitudes.

Hedin et al. [13] have reanalyzed the data used in the construction of MSIS. Spherical harmonic terms dependent on geographic latitude, longitude and universal time (UT) have been added to the previous expansion [2,3] which has not been modified. In such a way, a combined longitudinal/UT effect is introduced for the neutral temperature and composition. Longitudinal terms indicate a temperature enhancement of the order of 30 K near the magnetic poles. The universal time variation leads to an enhancement of the order of 30 K near 2130 UT in the northern hemisphere and nearly 70K around 0930 UT in the southern hemisphere. The combined longitude/UT effects lead to a rather complex pattern. As an example, Figs. 7 and 8 show the geographic distribution of ratios of the total density at 500 km between the modified model [13] and the initial model [2,3] for 3, 9, 15h and 21h UT respectively. Computations are made for $F = \bar{F} = 150 \times 10^{-22}$ Wm^{-2} Hz^{-1} and $A_p = 4$ under equinox conditions. The position of the sun is indicated on the equator by a small circle. It is clear that the universal time evolution of the longitudinal effect is a complex phenomenon which certainly needs further studies.

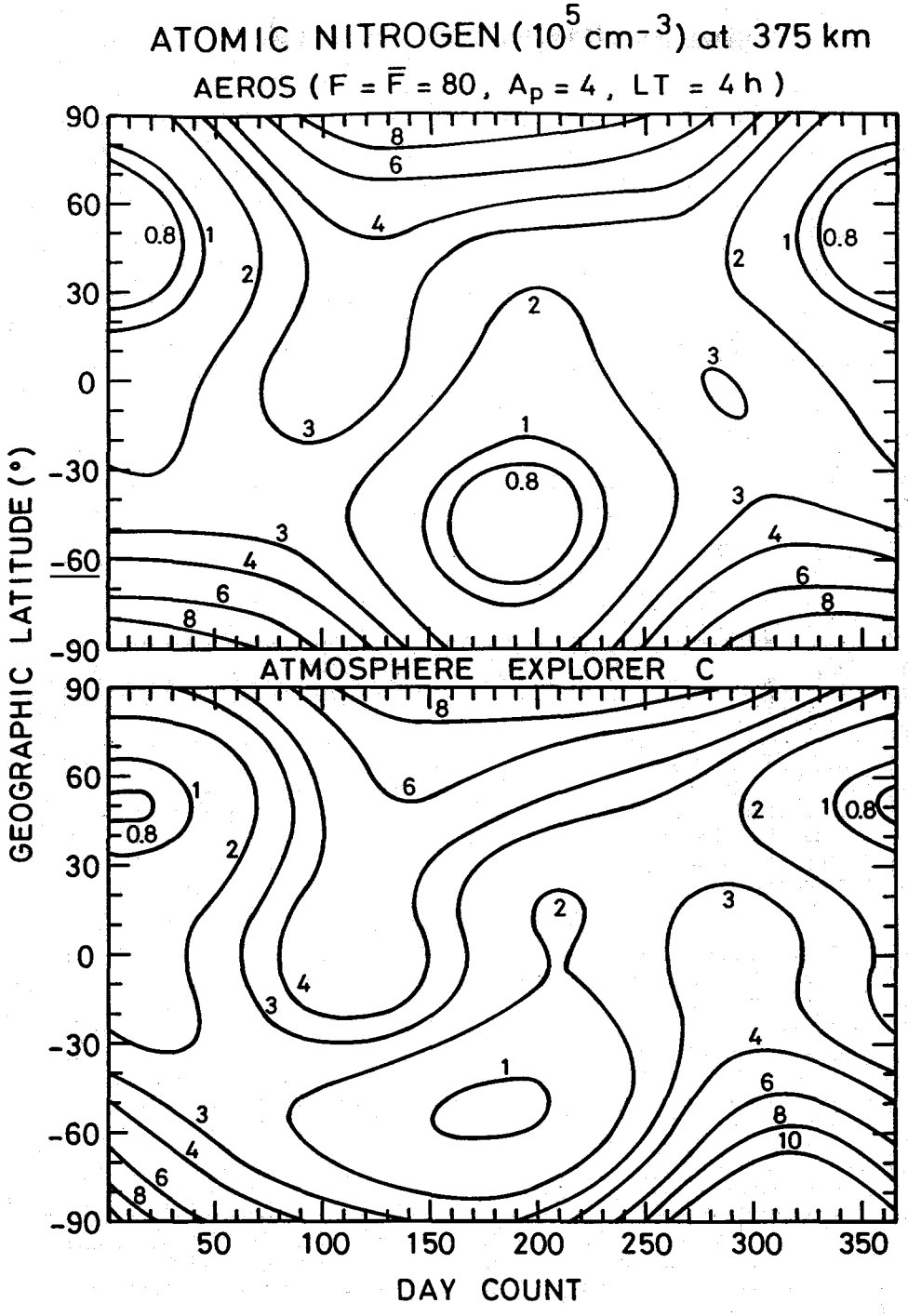

Fig. 5 Annual variation of atomic nitrogen at 375 km obtained at 4 hours LT for F = $\bar{F}$ = 80 x 10^{-22} Wm^{-2} Hz^{-1} and A_p = 4. Isopleths are in units of 10^5 cm^{-3}.

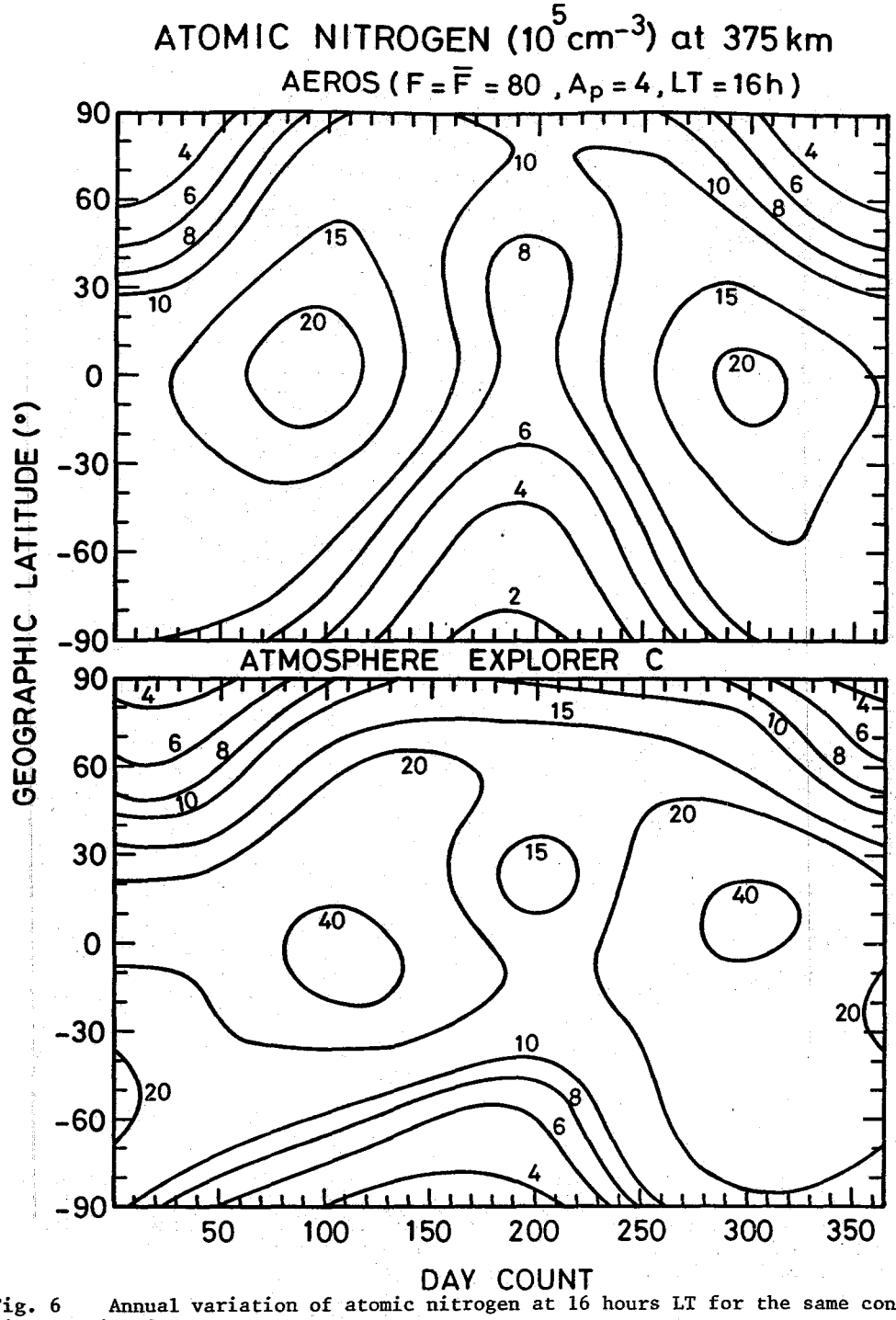

Fig. 6 Annual variation of atomic nitrogen at 16 hours LT for the same conditions as in Fig. 5.

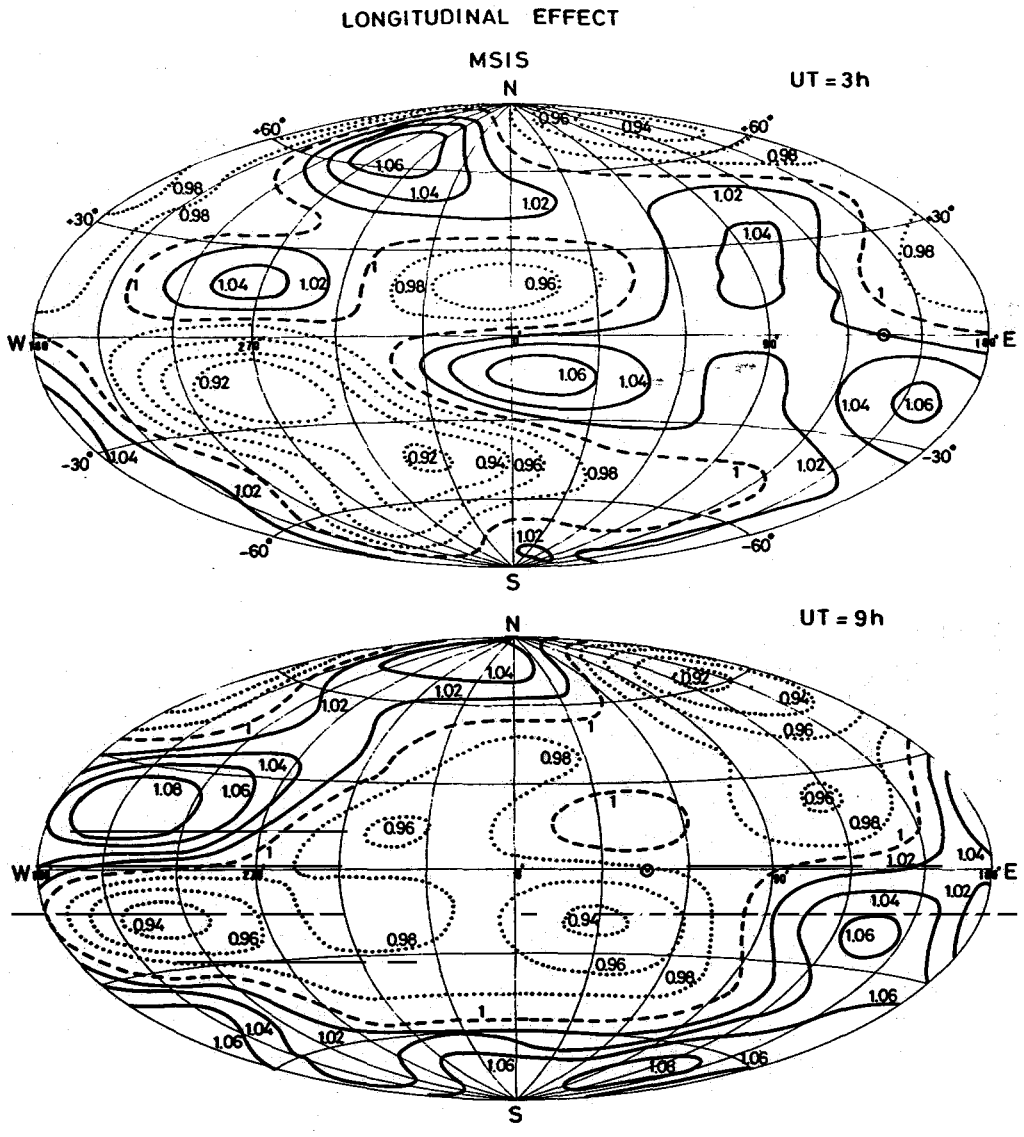

Fig. 7 Geographic distribution of the ratio between total densities at 500 km computed at equinox with and without longitudinal/UT effects in MSIS. Dotted isopleths correspond to ratios less than one and full isopleths to ratios greater than one. $F = \bar{F} = 150 \times 10^{-22}$ Wm^{-2} Hz^{-1} and $A_p = 4$. Upper part for 3 hours UT and lower part for 9 hours UT.

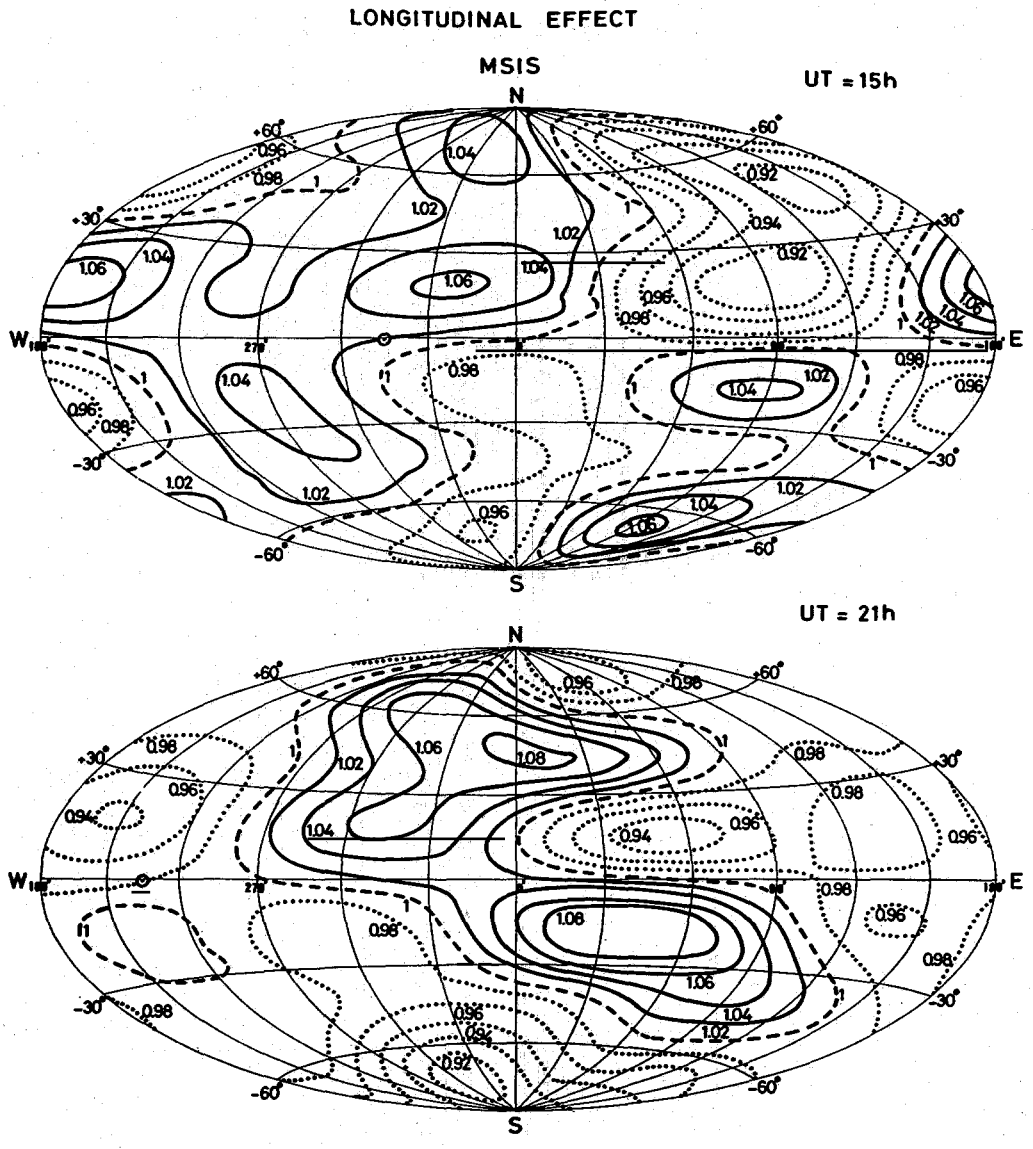

Fig. 8 Geographic distribution of longitudinal/UT effects for 15 hours and 21 hours UT. Same conditions as in Fig. 7.

A simpler approach has been undertaken by Laux and von Zahn [14] who introduced an empirical function for each atmospheric constituent of the ESRO 4 model [4]. These correction functions only depend on the geographic latitude and longitude. Possible universal time effects are, therefore, ignored and the temperature is not modified. Fig. 9 gives the longitudinal effect at 500 km on the total density in ESRO4 for the same solar and geomagnetic activities as in Figs 7 and 8. It should

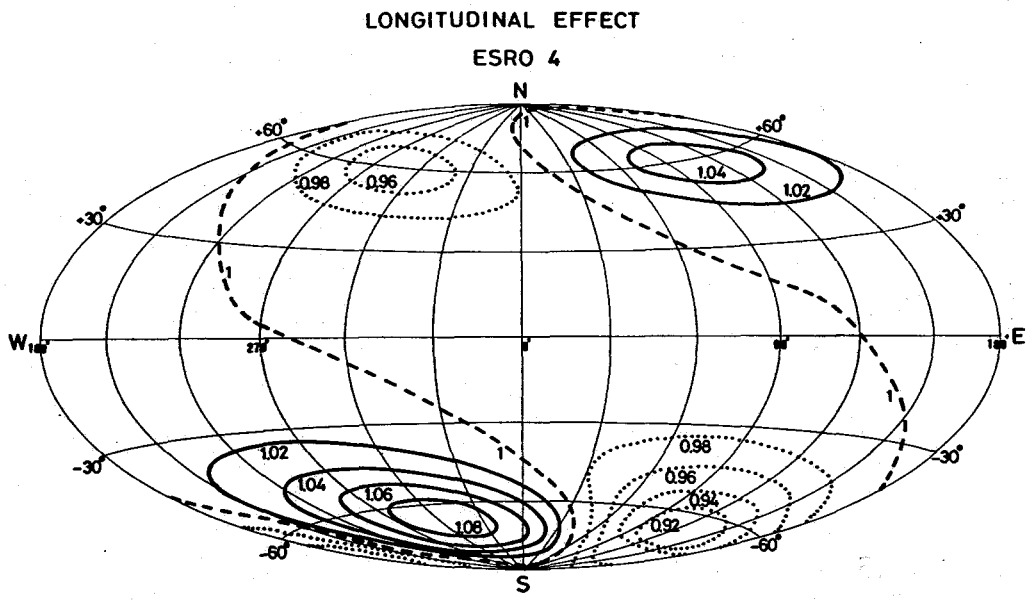

Fig. 9 Geographic distribution of longitudinal effects on the total density at 500 km in ESRO 4. $F = \bar{F} = 150$ Wm^{-2} Hz^{-1}, $A_p = 4$. Compare with Figs. 7 and 8.

be noted that the coefficient, C_7 for N_2 should be read 2.118×10^2 instead of 2.118 in Table 1 given by Laux and von Zahn [14]. Furthermore, the so-called "covariant latitude" is actually the colatitude which varies from 0° at the North pole to 180° at the South pole. The longitudinal effect for ESRO4 (Fig. 9) is completely different from the results given by MSIS (Figs 7 and 8). This is clearly shown in Fig. 10 where the total density ratio at 500 km is given as a function of longitude at ± 65° latitude for ESRO4 and for several universal times in MSIS. The maximum amplitude is of the order of ± 10% in both models but the phases never agree. ESRO4 can predict a density increase when MSIS leads to a Fig. 10 Total density density decrease. It is difficult to reconcile these two pictures unless the differences are entirely attributed to universal time effects not included in ESRO4. Although longitudinal variations are correlated to the configuration of the geomagnetic field, it appears that a consistent global representation is not yet entirely available. One should, however, realize that longitudinal/UT variations imply modifications of the order of a few percent, whereas it has been shown that differences of the order of a factor of two can still exist between total densities deduced from various models.

The various topics discussed in the present paper should not give the impression

of a poor knowledge of the thermospheric structure. In 1975, Jacchia 28 wrote : "the variations in the uppermost parts of the terrestrial atmosphere can be much better accounted for than can the weather in the atmospheric region in which we live !". Such a statement essentially refers to the total density and the recent semi-empirical models significantly contribute to the way this total

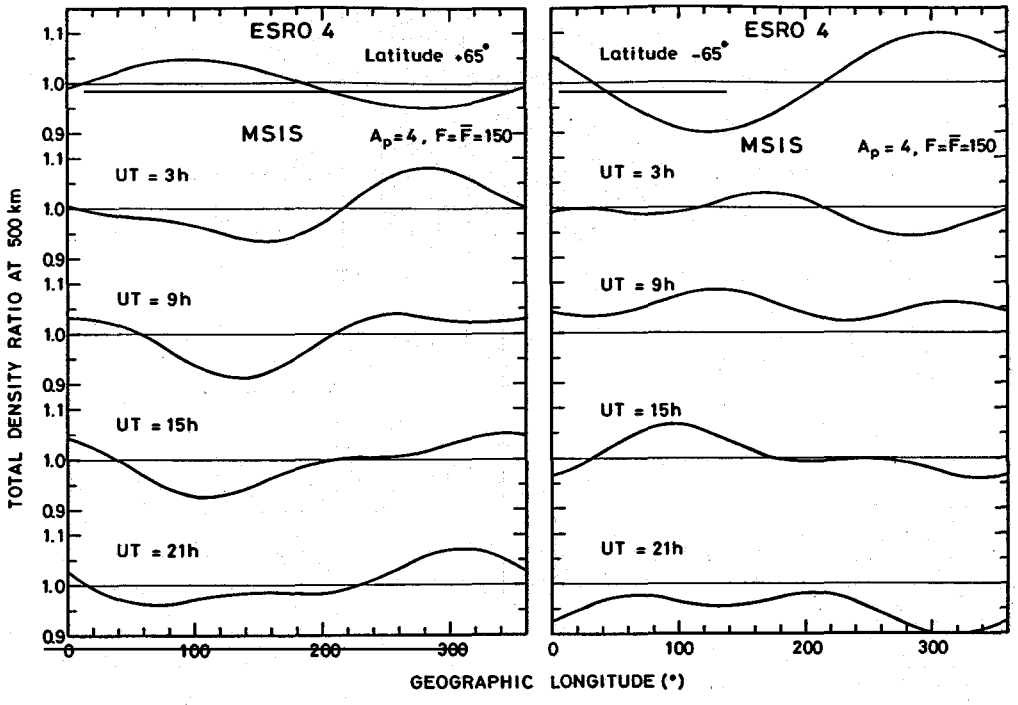

Fig. 10 Total density ratio at 500 km between models with and without longitudinal/UT effects at ± 65° geographic latitude. MSIS ratios are given for the same universal times as in Figs. 7 and 8.

density is built up. Important discrepancies still exist and it would be unwise to declare that experimental and theoretical research in the terrestrial upper atmosphere has reached a stage of development in which no fundamental discovery can be made.

References

1. CIRA 1972, Cospar International Reference Atmosphere, Akademie Verlag, Berlin, 1972.
2. A.E. Hedin, J.E. Salah, J.V. Evans, C.A. Reber, G.P. Newton, N.W. Spencer, D.E. Kayser, D. Alcaydé, P. Bauer, L. Cogger and J.P. McClure, J. Geophys. Res. 82, 2139 (1977).
3. A.E. Hedin, C.A. Reber, G.P. Newton, N.W. Spencer, H.C. Brinton and H.G. Mayr, J. Geophys. Res. 82, 2148 (1977).

4. U. von Zahn, W. Köhnlein, K.H. Fricke, U. Laux, H. Trinks and H. Volland, Geophys. Res. Lett. 4, 33 (1977).
5. L.G. Jacchia, Smithson. Astrophys. Obs. Spec. Rep. 375 (1977).
6. F. Barlier, C. Berger, J.L. Falin, G. Kockarts and G. Thuillier, Annls Géophys. 34, 9 (1978).
7. W. Köhnlein, D. Krankowsky, P. Lämmerzahl, W. Joos and H. Volland, J. Geophys. Res. 84, 4355 (1979).
8. A.E. Hedin, H.G. Mayr, C.A. Reber, N.W. Spencer and G.R. Carignan, J. Geophys. Res. 79, 215 (1974).
9. F. Barlier, C. Berger, J.L. Falin, G. Kockarts and G. Thuillier, J. Atmos. Terr. Phys. 41, 527 (1979).
10. L.G. Jacchia, Space Research XIX, 179 (1979).
11. L.G. Jacchia, Smithson. Astrophys. Obs. Spec. Rep. 332 (1971).
12. M.J. Engebretson, K. Mauersberger, D.C. Kayser, W.E. Potter and A.O. Nier; J. Geophys. Res 82, 461 (1977).
13. A.E. Hedin, C.A. Reber, N.W. Spencer, H.C. Brinton and D.C. Kayser, J. Geophys. Res. 84, 1 (1979).
14. U. Laux and U. von Zahn, J. Geophys. Res. 84, 1942 (1979).
15. D. Alcaydé, Space Research XIX, 211 (1979).
16. H. Trinks, U. von Zahn, C.A. Reber, A.E. Hedin, N.W. Spencer, D. Krankowsky, P. Lämmerzahl, D.C. Kayser and A.O. Nier, J. Geophys. Res. 82, 1261 (1977).
17. D.E. Anderson, Jr., R.R. Meier and C.S. Weller, J. Geophys. Res. 84, 1914 (1979).
18. D. Alcaydé and P. Bauer, Annls Géophys. 33, 305 (1977).
19. P.H.G. Dickinson, W.C. Bain, L. Thomas, E.R. Williams, D.B. Jenkins and N.D. Twiddy, Proc. Roy. Soc. Lond. A369, 379 (1980).
20. D. Alcaydé, J. Fontanari, G. Kockarts, P. Bauer and R. Bernard, Annls Géophys. 35, 41 (1979).
21. A.D. Danilov, U.A. Kalgin and A.A. Pokhunkov, Space Research XIX, 173 (1979).
22. H. Teitelbaum and J.E. Blamont, Planet. Space Sci. 25, 723 (1977).
23. S.P. Zimmerman and F.A. Murphy, in : Dynamical and Chemical Coupling between Neutral and Ionized Atmosphere (Grandal, B. and J.A. Holtet, eds), Reidel, Dordrecht, 1977, p. 35.
24. E.S. Oran, P.S. Julienne and D.F. Strobel, J. Geophys. Res. 80, 3068 (1975).
25. M.J. Engebretson, K. Mauersberger and W.E. Potter, J. Geophys. Res. 82, 3291 (1977).
26. G. Kockarts, Geophys. Res. Lett. 7, 137 (1980).
27. G. Thuillier, J.L. Falin and F. Barlier, J. Atmos. Terr. Phys. 42, to be published (1980).
28. L.G. Jacchia, Sky and Telescope 49, 294 (1975).